Asian Journal of Chemistry; Vol. 27, No. 10 (2015), 3543-3546

ASIAN JOURNAL OF CHEMISTRY

http://dx.doi.org/10.14233/ajchem.2015.18716

Upconversion Properties of $Y_2(MoO_4)_3:Er^{3+}/Yb^{3+}$ Particles Synthesized *via* Cyclic Microwave-Assisted Sol-Gel Route

CHANG SUNG LIM

Department of Advanced Materials Science and Engineering, Hanseo University, Seosan 356 706, Republic of Korea

Corresponding author: Tel/Fax: +82 41 6601445; E-mail: cslim@hanseo.ac.kr

Received: 8 September 2014; *Accepted*: 28 November 2014; *Published online*: 22 June 2015; AJC-17298

Green phosphors of $Y_{2-x}(MoO_4)_3:Er^{3+}/Yb^{3+}$ with doping concentrations of Er^{3+} and Yb^{3+} ($x = Er^{3+} + Yb^{3+}$, $Er^{3+} = 0.05, 0.1, 0.2$ and $Yb^{3+} = 0.2, 0.45$) were synthesized *via* the cyclic microwave-assisted sol-gel route and their upconversion properties were investigated. Well-crystallized particles, formed after heat-treatment at 900 °C for 16 h, showed a fine and homogeneous morphology with particle sizes of 5-10 μm. Under excitation at 980 nm, $Y_2(MoO_4)_3:Er^{3+}/Yb^{3+}$ particles exhibited a strong 525 nm and a weak 550 nm emission bands in the green region and a very weak 655 nm emission band in the red region. Raman spectra of the particles indicated the presence of strong peaks at both higher frequencies and lower frequencies induced by the disorder of the $[MoO_4]^{2-}$ groups with the incorporation of the Er^{3+} and Yb^{3+} elements into the crystal lattice or by a new phase formation.

Keywords: Upconversion, Green Phosphors, Microwave sol-gel, Raman spectroscopy.

INTRODUCTION

Rare-earth doped upconversion (UC) phosphors with unique optical properties have great potential applications in the fields of lasers, three-dimensional displays, light-emitting devices and biological detectors[1,2]. Recently, the synthesis and the luminescence properties of upconversion particles have attracted considerable interest since they are considered as potentially active components in new optoelectronic devices and luminescent labels for imaging and bio-detection assays, which overcome the current limitations in traditional photoluminescence materials[3]. It is possible that the trivalent rare- earth ions in the disordered structure could be partially substituted by Er^{3+} and Yb^{3+} ions and the ions are effectively doped into the crystal lattices due to the similar radii of trivalent rare-earth ions, resulted in the excellent upconversion photoluminescence properties[4-7]. Among the rare-earth ions, the Er^{3+} ion is suitable for converting infrared to visible light through the upconversion process due to proper electronic energy level configuration. The co-doped Yb^{3+} ion and Er^{3+} ion can remarkably enhance the upconversion efficiency from infrared to visible light due to the efficiency energy transfer from Yb^{3+} to Er^{3+}. The Yb^{3+} ion as a sensitizer can be effectively excited by incident light source energy that is transferred to the activator, from which radiation can be emitted. The Er3+ ion activator is the luminescence center of the upconversion particles, while the sensitizer enhances the upconversion luminescence efficiency[8-10].

For practical application of upconversion photoluminescence in products, the features such as homogeneous upconversion particle size distribution and morphology need to be well defined. Usually, molybdates are prepared by a solid-state method that requires high temperatures, lengthy heating process and subsequent grinding, which results in loss of the emission intensity. Sol-gel process has some advantages including good homogeneity, low calcination temperature and small particle size and narrow particle size distribution for good luminescent characteristics. However, the sol-gel process has a disadvantage in that it takes a long time for gelation. As compared with the usual methods, microwave-assisted sol-gel synthesis has the advantages of short reaction time, homogeneous morphology features and high purity of final polycrystalline samples[11-13]. Microwave heating is delivered to the material surface by radiant and/or convection heating, which is transferred to the bulk of the material *via* conduction[14,15]. A cyclic microwave-assisted sol-gel process is a cost-effective method that provides high homogeneity with easy scale-up and it is emerging as a viable alternative approach for the synthesis of high-quality luminescent materials in short time periods. However, the cyclic microwave-assisted sol-gel process of $Y_2(MoO_4)_4:Er^{3+}/Yb^{3+}$ phosphors has not been reported yet.

In this study, $Y_{2-x}(MoO_4)_4:Er^{3+}/Yb^{3+}$ phosphors with doping concentrations of Er^{3+} and Yb^{3+} ($x = Er^{3+} + Yb^{3+}$, $Er^{3+} = 0.05, 0.1, 0.2$ and $Yb^{3+} = 0.2, 0.45$) were synthesized *via* the cyclic microwave-assisted sol-gel route. The synthesized

particles were characterized by X-ray diffraction (XRD), scanning electron microscopy (SEM) and energy-dispersive X-ray spectroscopy (EDS). The optical properties were examined comparatively using photoluminescence (PL) emission and Raman spectroscopy.

EXPERIMENTAL

Appropriate stoichiometric amounts of $Y(NO_3)_3 \cdot 6H_2O$ (99 %, Sigma-Aldrich, USA), $(NH_4)_6Mo_7O_{24} \cdot 4H_2O$ (99 %, Alfa Aesar, USA), $Er(NO_3)_3 \cdot 5H_2O$ (99.9 %, Sigma-Aldrich, USA), $Yb(NO_3)_3 \cdot 5H_2O$ (99.9 %, Sigma-Aldrich, USA), citric acid (99.5 %, Daejung Chemicals, Korea), NH_4OH (A.R.), ethylene glycol (A.R.) and distilled water were used to prepare $Y_2(MoO_4)_3$, $Y_{1.8}(MoO_4)_3$:$Er_{0.2}$, $Y_{1.7}(MoO_4)_3$:$Er_{0.1}Yb_{0.2}$ and $Y_{1.5}(MoO_4)_3$:$Er_{0.05}Yb_{0.45}$ compounds with doping concentrations of Er^{3+} and Yb^{3+} (Er^{3+} = 0.05, 0.1, 0.2 and Yb^{3+} = 0.2, 0.45). To prepare $Y_2(MoO_4)_3$, 0.4 mol % $Y(NO_3)_2 \cdot 6H_2O$ and 0.17 mol % $(NH_4)_6Mo_7O_{24} \cdot 4H_2O$ were dissolved in 20 mL of ethylene glycol and 80 mL of 5M NH_4OH under vigorous stirring and heating. Subsequently, citric acid (with a molar ratio of citric acid to total metal ions of 2:1) was dissolved in 100 mL of distilled water under vigorous stirring and heating. Then, the solutions were mixed together under vigorous stirring and heating at 80-100 °C. At the end, highly transparent solutions were obtained and adjusted to pH = 7-8 by the addition of NH_4OH or citric acid.

In order to prepare $Y_{1.8}(MoO_4)_3$:$Er_{0.2}$, the mixture of 0.72 mol % $Y(NO_3)_3 \cdot 6H_2O$ with 0.08 mol % $Er(NO_3)_3 \cdot 5H_2O$ was used for the rare earth solution. In order to prepare $Y_{1.7}(MoO_4)_3$:$Er_{0.1}Yb_{0.2}$, the mixture of 0.68 mol % $Y(NO_3)_3 \cdot 6H_2O$ with 0.04 mol % $Er(NO_3)_3 \cdot 5H_2O$ and 0.08 mol % $Yb(NO_3)_3 \cdot 5H_2O$ was used for the rare earth solution. In order to prepare $Y_{1.5}(MoO_4)_3$:$Er_{0.05}Yb_{0.45}$, the rare-earth containing solution was generated using 0.6 mol % $Y(NO_3)_3 \cdot 6H_2O$ with 0.02 mol % $Er(NO_3)_3 \cdot 5H_2O$ and 0.18 mol % $Yb(NO_3)_3 \cdot 5H_2O$.

The transparent solutions were placed into a microwave oven operating at a frequency of 2.45 GHz with a maximum output-power of 1250 W for 0.5 h. The working cycle of the microwave reaction was controlled precisely using a regime of 40 s on and 20 s off for 15 min, followed by further treatment of 30 s on and 30 s off for 15 min. The samples were treated with ultrasonic radiation for 10 min to produce a light yellow transparent sol. After this, the light yellow transparent sols were dried at 120 °C in a dry oven to obtain black dried gels. The black dried gels were grinded and heat-treated at 900 °C for 16 h with 100 °C intervals between 600-900 °C. Finally, white particles were obtained for $Y_2(MoO_4)_3$ and pink particles for the doped compositions.

The phase composition of the synthesized particles was identified using XRD (D/MAX 2200, Rigaku, Japan). The microstructure and surface morphology of the synthesized particles were observed using SEM/EDS (JSM-5600, JEOL, Japan). The PL spectra were recorded using a spectrophotometer (Perkin Elmer LS55, UK) at room temperature. Raman spectroscopy measurements were performed using a LabRam Aramis (Horiba Jobin-Yvon, France). The 514.5 nm line of an Ar ion laser was used as the excitation source and the power on the samples was kept at 0.5 mW.

RESULTS AND DISCUSSION

Fig. 1 shows the XRD patterns of the (a) JCPDS 28-1451 data of $Y_2(MoO_4)_3$, the synthesized (b) $Y_{1.8}(MoO_4)_3$:$Er_{0.2}$, (c) $Y_{1.7}(MoO_4)_3$:$Er_{0.1}Yb_{0.2}$ and (d) $Y_{1.5}(MoO_4)_3$:$Er_{0.05}Yb_{0.45}$ particles. The crystal structures are in good agreement with the crystallographic data of $Y_2(MoO_4)_3$ (JCPDS 28-1461)[16,17]. The obtained samples are effectively incorporated into the $Y_2(MoO_4)_3$ crystal lattice after partial substitution of Y^{3+} by Er^{3+} and Yb^{3+} ions. This suggests that the cyclic microwave-assisted sol-gel route is suitable for the growth of $Y_{2-x}(MoO_4)_3$:Er^{3+}/Yb^{3+} crystallites. Post heat-treatment plays an important role in a well-defined crystallized morphology. To achieve a well-defined crystalline morphology, $Y_2(MoO_4)_3$, $Y_{1.8}(MoO_4)_3$:$Er_{0.2}$, $Y_{1.7}(MoO_4)_3$:$Er_{0.1}Yb_{0.2}$ and $Y_{1.5}(MoO_4)_3$: $Er_{0.05}Yb_{0.45}$ phases need to be heat treated at 900 °C for 16 h. It is assumed that the doping amount of Er^{3+}/Yb^{3+} has a great effect on the crystalline cell volume of the $Y_2(MoO_4)_3$, because of the different ionic sizes and energy band gaps. This means that the obtained samples are effectively doped into crystal lattices of the $Y_2(MoO_4)_3$ phase due to the similar radii of Y^{3+}, Er^{3+} and Yb^{3+}.

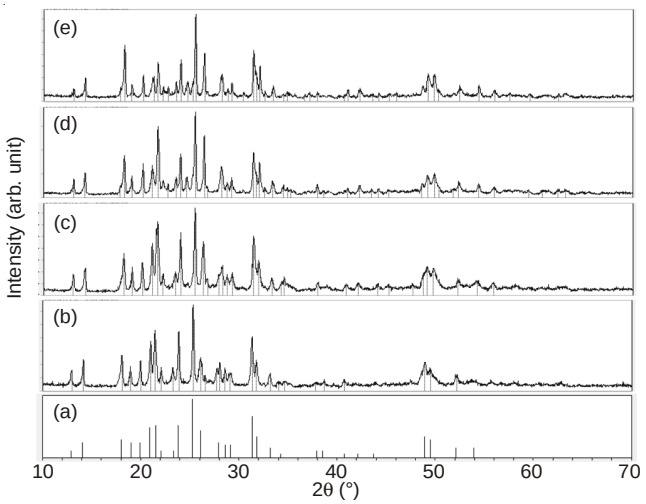

Fig. 1. X-ray diffraction patterns of the (a) JCPDS 28-1451 data of $Y_2(MoO_4)_3$, the synthesized (b) $Y_{1.8}(MoO_4)_3$:$Er_{0.2}$, (c) $Y_{1.7}(MoO_4)_3$:$Er_{0.1}Yb_{0.2}$ and (d) $Y_{1.5}(MoO_4)_3$:$Er_{0.05}Yb_{0.45}$ particles

Fig. 2 shows a SEM image of the synthesized $Y_{1.5}(MoO_4)_3$:$Er_{0.05}Yb_{0.45}$ particles. The as-synthesized samples are well crystallized with a fine and homogeneous morphology and particle size of 5-10 μm. Fig. 3 shows the energy-dispersive X-ray spectroscopy patterns of the synthesized (a) $Y_{0.7}(MoO_4)_3$:$Er_{0.1}Yb_{0.2}$ and (b) $Y_{0.5}(MoO_4)_3$:$Er_{0.05}Yb_{0.45}$ particles and quantitative compositions of (c) $Y_{0.7}(MoO_4)_3$:$Er_{0.1}Yb_{0.2}$ and (d) $Y_{0.5}(MoO_4)_3$:$Er_{0.05}Yb_{0.45}$ particles. The EDS pattern shows that the (a) $Y_{0.7}(MoO_4)_3$:$Er_{0.1}Yb_{0.2}$ and (b) $Y_{0.5}(MoO_4)_3$:$Er_{0.05}Yb_{0.45}$ particles are composed of Y, Mo, O and Er for $Y_{0.7}(MoO_4)_3$:$Er_{0.1}Yb_{0.2}$ and Y, Mo, O, Er and Yb for $Y_{0.5}(MoO_4)_3$:$Er_{0.05}Yb_{0.45}$ particles. The quantitative compositions of (c) and (d) are in good relation with nominal compositions of the particles. The relation of Y, Mo, O, Er and Yb components exhibit that $Y_{0.7}(MoO_4)_3$:$Er_{0.1}Yb_{0.2}$ and $Y_{0.5}(MoO_4)_3$:$Er_{0.05}Yb_{0.45}$ particles can be successfully synthesized using the cyclic microwave-assisted sol-gel method. The cyclic microwave-assisted sol-gel route of the molybdates provides the energy to synthesize

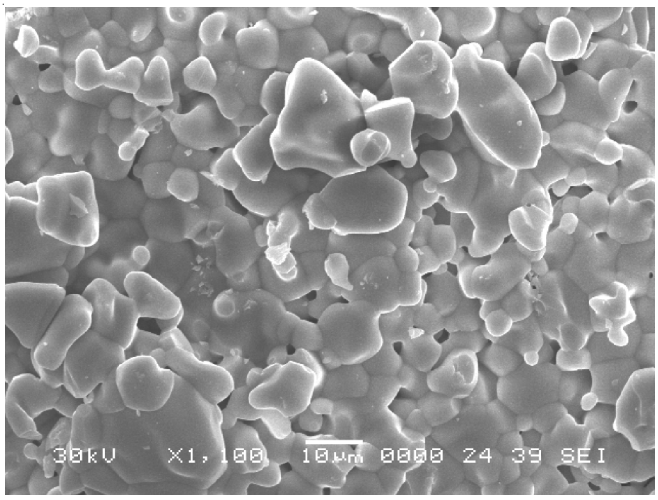

Fig. 2. Scanning electron microscopy image of the synthesized $Y_{1.5}(MoO_4)_3:Er_{0.05}Yb_{0.45}$ particles

(a)

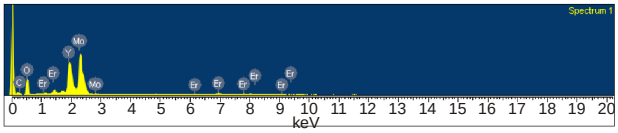

(b)

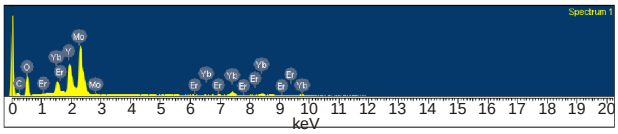

(c)

Spectrum	In stats.	C	O	Y	Mo	Er	Total
Spectrum 1	Yes	13.49	40.23	14.90	28.10	3.28	100.00
Spectrum 2	Yes	18.88	38.51	13.58	26.03	3.00	100.00
Spectrum 3	Yes	13.92	40.08	14.75	28.12	3.13	100.00
Spectrum 4	Yes	3.90	43.34	17.07	31.81	3.88	100.00
Mean		12.55	40.54	15.07	28.51	3.32	100.00
Std. deviation		6.26	2.02	1.45	2.41	0.39	
Max.		18.88	43.34	17.07	31.81	3.88	
Min.		3.90	38.51	13.58	26.03	3.00	

(d)

Spectrum	In stats.	C	O	Y	Mo	Er	Yb	Total
Spectrum 1	Yes	5.79	39.94	13.18	31.10	0.75	9.25	100.00
Spectrum 2	Yes	7.83	39.65	12.50	30.19	0.68	9.15	100.00
Spectrum 3	Yes	3.28	41.98	13.08	31.29	0.55	9.82	100.00
Spectrum 4	Yes	5.58	40.81	12.90	30.97	0.76	8.97	100.00
Mean		5.62	40.59	12.92	30.89	0.69	9.30	100.00
Std. deviation		1.86	1.05	0.30	0.48	0.10	0.37	
Max.		7.83	41.98	13.18	31.29	0.76	9.82	
Min.		3.28	39.65	12.50	30.19	0.55	8.97	

Fig. 3. Energy-dispersive X-ray spectroscopy patterns of the synthesized (a) $Y_{0.7}(MoO_4)_3:Er_{0.1}Yb_{0.2}$ and (b) $Y_{0.5}(MoO_4)_3:Er_{0.05}Yb_{0.45}$ particles, and quantitative compositions of (c) $Y_{0.7}(MoO_4)_3:Er_{0.1}Yb_{0.2}$ and (d) $Y_{0.5}(MoO_4)_3:Er_{0.05}Yb_{0.45}$ particles

the bulk of the material uniformly, so that fine particles with controlled morphology can be fabricated in a short time period. The method is a cost-effective way to provide highly homogeneous products and is easy to scale-up, it is a viable alternative for the rapid synthesis of upconversion particles.

Fig. 4 shows the upconversion photoluminescence emission spectra of the as-prepared (a) $Y_2(MoO_4)_3$, (b) $Y_{1.8}(MoO_4)_3:Er_{0.2}$, (c) $Y_{1.7}(MoO_4)_3:Er_{0.1}Yb_{0.2}$ and (d) $Y_{1.5}(MoO_4)_3:Er_{0.05}Yb_{0.45}$ particles excited under 980 nm at room temperature. The upconversion intensities of (c) $Y_{1.7}(MoO_4)_3:Er_{0.1}Yb_{0.2}$ and (d) $Y_{1.5}(MoO_4)_3:Er_{0.05}Yb_{0.45}$ particles exhibited a strong 525 nm emission band, a weak 550 nm emission band in the green region and a very weak 655 nm emission band in the red region. The strong 525 nm emission band and the weak 550 nm emission band in the green region corresponds to the $^2H_{11/2} \rightarrow {}^4I_{15/2}$ and $^4S_{3/2} \rightarrow {}^4I_{15/2}$ transitions, respectively, while the weak emission 655 nm band in the red region corresponds to the

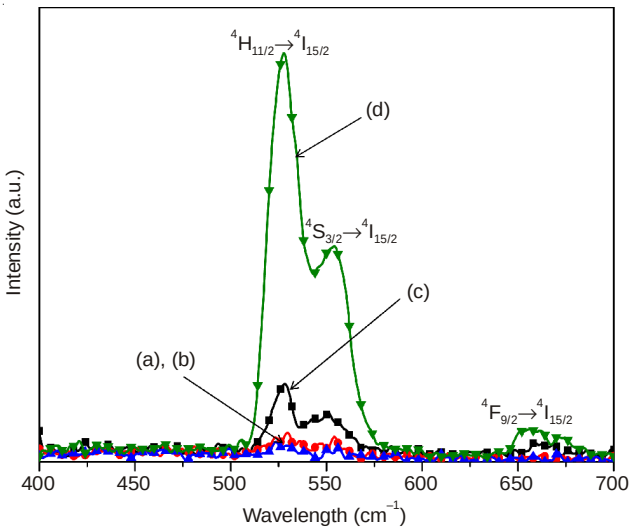

Fig. 4. Upconversion photoluminescence emission spectra of (a) $Y_2(MoO_4)_3$, (b) $Y_{1.8}(MoO_4)_3:Er_{0.2}$, (c) $Y_{1.7}(MoO_4)_3:Er_{0.1}Yb_{0.2}$ and (d) $Y_{1.5}(MoO_4)_3:Er_{0.05}Yb_{0.45}$ particles excited under 980 nm at room temperature

$^4F_{9/2} \rightarrow {}^4I_{15/2}$ transition. The upconversion intensities of $Y_2(MoO_4)_3$ and (b) $Y_{1.8}(MoO_4)_3:Er_{0.2}$, were not detected. The upconversion intensity of (d) $Y_{1.5}(MoO_4)_3:Er_{0.05}Yb_{0.45}$ is much higher than those of (c) $Y_{1.7}(MoO_4)_3:Er_{0.1}Yb_{0.2}$ particles. Similar results are also observed from Er^{3+}/Yb^{3+} co-doped in other host matrices, which are assigned to the upconversion emission spectra with the green emission intensity ($^2H_{11/2} \rightarrow {}^4I_{15/2}$ and $^4S_{3/2} \rightarrow {}^4I_{15/2}$ transitions) and the red emission intensity ($^4F_{9/2} \rightarrow {}^4I_{15/2}$ transition)[18-22]. The doping amounts of Er^{3+}/Yb^{3+} had a great effect on the morphological features of the particles and their upconversion fluorescence intensity. The Yb^{3+} ion sensitizer can be effectively excited by the energy of an incident light source, this energy is transferred to the activator where radiation can be emitted. The Er^{3+} ion activator is the luminescence center for these upconversion particles and the sensitizer enhances the upconversion luminescence efficiency. This process requires the absorption of two or more photons to produce sufficient energy for upconversion emission. The much higher intensity of the $^2H_{11/2} \rightarrow {}^4I_{15/2}$ transition in comparison with the $^4S_{3/2} \rightarrow {}^4I_{15/2}$ transition in Fig. 4 may be induced by the concentration quenching effect due to the energy transfer between the nearest Er^{3+} and Yb^{3+} ions and the interactions between doping ions in the $Y_{2-x}(MoO_4)_3$ host matrix. This means that the green band $^2H_{11/2} \rightarrow {}^4I_{15/2}$ transitions are assumed to be more easily quenched than the $^4S_{3/2} \rightarrow {}^4I_{15/2}$ transition by non-radiative relaxation in the case of the host matrix.

Fig. 5 shows the Raman spectra of the synthesized (a) $Y_2(MoO_4)_3$(YM), (b) $Y_{1.8}(MoO_4)_3:Er_{0.2}$(YM:Er), (c) $Y_{1.7}(MoO_4)_3:Er_{0.1}Yb_{0.2}$(YM:ErYb) and (d) $Y_{1.5}(MoO_4)_3:Er_{0.05}Yb_{0.45}$ (YM:ErYb#) particles excited by the 514.5 nm line of an Ar ion laser at 0.5 mW. The well-resolved sharp peaks for the (a) $Y_2(MoO_4)_3$ particles indicate a high crystallinity state of the synthesized particles. The internal vibration mode frequencies are dependent on the lattice parameters and the degree of the partially covalent bond between the cation and molecular ionic group $[MoO_4]^{2-}$. The Raman spectra of the (b) $Y_{1.8}(MoO_4)_3:Er_{0.2}$(YM:Er), (c) $Y_{1.7}(MoO_4)_3:Er_{0.1}Yb_{0.2}$(YM:ErYb) and (d) $Y_{1.5}(MoO_4)_3:Er_{0.05}Yb_{0.45}$(YM:ErYb#) particles indicate the

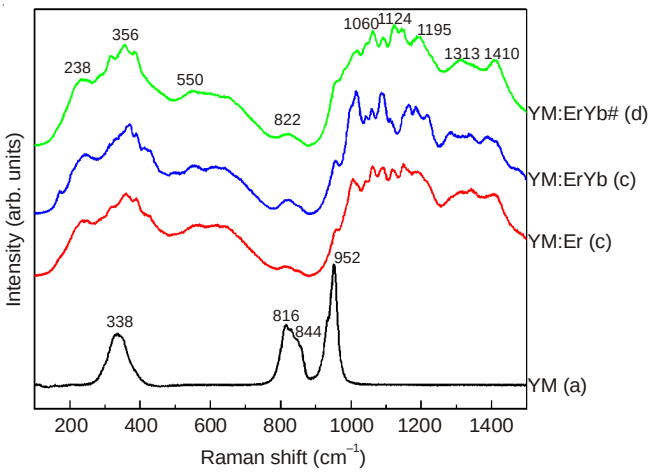

Fig. 5. Raman spectra of the synthesized (a) $Y_2(MoO_4)_3$(YM), (b) $Y_{1.8}(MoO_4)_3$:$Er_{0.2}$(YM:Er), (c) $Y_{1.7}(MoO_4)_3$:$Er_{0.1}Yb_{0.2}$(YM:ErYb) and (d) $Y_{1.5}(MoO_4)_3$:$Er_{0.05}Yb_{0.45}$(YM:ErYb#) particles excited by the 514.5-nm line of an Ar ion laser at 0.5 mW

domination of the strong peaks at higher frequencies of 822, 1060, 1124, 1195, 1313 and 1410 cm^{-1} and the weak peaks at lower frequencies of 238, 356 and 550 cm^{-1}. The Raman spectra of the doped particles prove that the doping ions can influence the structure of the host materials. The combination of a heavy metal cation and the large inter-ionic distance for Er^{3+} and Yb^{3+} substitutions in Y^{3+} sites in the lattice result in a high probability of upconversion and phonon-splitting relaxation in $Y_{2-x}(MoO_4)_3$ crystals. It may be that these very strong and strange effects are generated by the disorder of the $[MoO_4]^{2-}$ groups with the incorporation of the Er^{3+} and Yb^{3+} elements into the crystal lattice or by a new phase formation.

Conclusion

The green phosphors of $Y_{2-x}(MoO_4)_3$:Er^{3+}/Yb^{3+} with doping concentrations of Er^{3+} and Yb^{3+} (x = Er^{3+} + Yb^{3+}, Er^{3+} = 0.05, 0.1, 0.2 and Yb^{3+} = 0.2, 0.45) were successfully synthesized *via* the cyclic microwave-assisted sol-gel route. Well-crystallized particles formed after heat-treatment at 900 °C for 16 h showed a fine and homogeneous morphology with particle sizes of 5-10 μm. Under excitation at 980 nm, the upconversion intensities of $Y_{1.7}(MoO_4)_3$:$Er_{0.1}Yb_{0.2}$ and $Y_{1.5}(MoO_4)_3$:$Er_{0.05}Yb_{0.45}$ particles exhibited a strong 525 nm emission band and a weak 550 nm emission band in the green region, which were assigned to the $^2H_{11/2} \rightarrow {}^4I_{15/2}$ and $^4S_{3/2} \rightarrow {}^4I_{15/2}$ transitions, respectively, while a very weak 655 nm emission band in the red region was assigned to the $^4F_{9/2} \rightarrow {}^4I_{15/2}$ transition. The upconversion intensity of $Y_{1.5}(MoO_4)_3$: $Er_{0.05}Yb_{0.45}$ particles was much higher than that of the $Y_{1.7}(MoO_4)_3$:$Er_{0.1}Yb_{0.2}$ particles. The Raman spectra of the doped particles indicated the domination of the strong peaks at higher frequencies of 822, 1060, 1124, 1195, 1313 and 1410 cm^{-1} and the weak peaks at lower frequencies of 238, 356 and 550 cm^{-1} generated by the disorder of the $[MoO_4]^{2-}$ groups with the incorporation of the Er^{3+} and Yb^{3+} elements into the crystal lattice or by a new phase formation.

ACKNOWLEDGEMENTS

This study was supported by the Basic Science Research Program through the National Research Foundation of Korea (NRF) funded by the Ministry of Science, ICT & Future Planning (2014-046024).

REFERENCES

1. M. Lin, Y. Zhao, S.Q. Wang, M. Liu, Z.F. Duan, Y.M. Chen, F. Li, F. Xu and T.J. Lu, *Biotechnol. Adv.*, **30**, 1551 (2012).
2. M. Wang, G. Abbineni, A. Clevenger, C. Mao and S. Xu, *Nanomedicine*, **7**, 710 (2011).
3. A. Shalav, B.S. Richards and M.A. Green, *Sol. Energy Mater. Sol. Cells*, **91**, 829 (2007).
4. C.S. Lim and V.V. Atuchin, *Proc. SPIE*, **8771**, 877110 (2013).
5. J. Liao, D. Zhou, B. Yang, R. Liu, Q. Zhang and Q. Zhou, *J. Lumin.*, **134**, 533 (2013).
6. J. Sun, J. Xian and H. Du, *J. Phys. Chem. Solids*, **72**, 207 (2011).
7. C. Guo, H.K. Yang and J.H. Jeong, *J. Lumin.*, **130**, 1390 (2010).
8. V.K. Komarala, Y. Wang and M. Xiao, *Chem. Phys. Lett.*, **490**, 189 (2010).
9. J. Sun, J. Xian, Z. Xia and H. Du, *J. Rare Earths*, **28**, 219 (2010).
10. J.Y. Sun, Y.J. Lan, Z.G. Xia and H.Y. Du, *Opt. Mater.*, **33**, 576 (2011).
11. J. Yao, Z. Jia, P. Zhang, C. Shen, J. Wang, K.F. Aguey-Zinsou, C. Ma and L. Wang, *Ceram. Int.*, **39**, 2165 (2013).
12. Z. Xia, H. Du, J. Sun, D. Chen and X. Wang, *Mater. Chem. Phys.*, **119**, 7 (2010).
13. F. Wu, L. Wang, C. Wu and Y. Bai, *Electrochim. Acta*, **54**, 4613 (2009).
14. C.S. Lim, *Mater. Chem. Phys.*, **140**, 154 (2013).
15. C.S. Lim, *Asian J. Chem.*, **25**, 63 (2013).
16. W. Lu, L. Cheng, J. Sun, H. Zhong, X. Li, Y. Tian, J. Wan, Y. Zheng, L. Huang, T. Yu, H. Yu and B. Chen, *Physica B*, **405**, 3284 (2010).
17. Y. Tian, B. Chen, B. Tian, R. Hua, J. Sun, L. Cheng, H. Zhong, X. Li, J. Zhang, Y. Zheng, T. Yu, L. Huang and Q. Meng, *J. Alloys Comp.*, **509**, 6096 (2011).
18. C. Guo, T. Chen, L. Luan, W. Zhang and D. Huang, *J. Phys. Chem. Solids*, **69**, 1905 (2008).
19. H. Du, Y. Lan, Z. Xia and J. Sun, *Mater. Res. Bull.*, **44**, 1660 (2009).
20. C.S. Lim, *Mater. Res. Bull.*, **47**, 4220 (2012).
21. W. Lu, L. Cheng, J. Sun, H. Zhong, X. Li, Y. Tian, J. Wan, Y. Zheng, L. Huang, T. Yu, H. Yu and B. Chen, *Physica B*, **405**, 3284 (2010).
22. J. Sun, J. Xian, X. Zhang and H. Du, *J. Rare Earths*, **29**, 32 (2011).